Early Warning Analysis of Grid Ferromagnetic Resonance Overvoltage Risk Based on Multi-source Data

Gou Yu

College of Electrical Engineering & New Energy at China Three Gorges University, Yichang Hubei 443002, China
E-mail: gouyuu04@ctgu.edu.cn

Received 27 May 2023; Accepted 26 June 2023;
Publication 26 August 2023

Abstract

In the impartial factor ungrounded system, ferromagnetic resonance overvoltage is a frequent fault that lasts for a lengthy time and is hazardous to the grid. In this paper, the mechanism of grid ferromagnetic resonance overvoltage is first explored in depth. The precept of impartial voltage shift and ferromagnetic resonance brought about through PT saturation is analyzed with the aid of graphical and mathematical analysis. Then, the characteristics of fault current information are extracted by wavelet transform, and indicators such as wavelet fault degree, wavelet singularity and wavelet energy measurement are obtained respectively. D-S evidence theory is used to fuse multi-source information of electrical volume and switching quantity, so as to obtain comprehensive fault results of power grid more accurately. Finally, based on the time series risk assessment, the distribution network time series risk index is calculated, the risk level and risk area of each period are determined, and

Distributed Generation & Alternative Energy Journal, Vol. 38_6, 1763–1790.
doi: 10.13052/dgaej2156-3306.3863

the early warning results are issued. Finally, an example is given to verify the effectiveness of the proposed method.

Keywords: Distribution network, ferromagnetic resonance overvoltage, multi-source data, risk warning.

1 Introduction

Smart grid is the future improvement course of the world's electricity grid, and its vital characteristic is "self-healing", which requires the grid to be in a position to analyze and consider the gadget protection online, in actual time and continuously, to be in a position to diagnose the machine on line and to be in a position to warn the viable gadget failure in time, to be capable to prevent, isolate and manipulate the gadget failure that has already occurred, and to make the machine self-healing [1, 2]. The device is in a position to prevent, isolate and manipulate gadget faults that have already occurred, so that the machine can get better itself and allow shut coordination between all ranges of the grid defense, which can withstand surprising occasions and serious faults and efficiently keep away from the incidence of large-scale chain faults, as a result substantially enhancing the protection and balance of the grid and electricity grant reliability, and notably decreasing outage losses.

Ferromagnetic resonance happens in nonlinear inductive and capacitive circuits, and the resonance method can also produce steady overvoltage and overcurrent, which will pose a danger to the protection of transmission and distribution gear and running personnel. Although a lot of lookups have been carried out at domestic and overseas on the era mechanism, primary characteristics, improvement law, and suppression measures of ferromagnetic resonance, due to the complexity of its resonance circuit and the variety of resonance types, the suppression measures of ferromagnetic resonance are limited [3]. However, due to the complexity of the resonant circuit and the variety of resonant types, ferromagnetic resonance suppression measures are restrained in some resonant cases, ensuing in the key gear of the strength gadget may also be subjected to a longer length of ferromagnetic resonance overvoltage, which can also reason insulation injury and finally might also reason tools damage, as a result, the ferromagnetic resonance trouble is nonetheless a complicated hassle that has plagued the protected operation of electricity gadget for a lengthy time [4]. With the development of the power grid, on the one hand, the rapid development of the distribution network causes a sharp increase in the range of distribution system parameter

changes, and the distribution network operation is more frequent, prompting the occurrence rate of ferromagnetic resonance to rise; on the other hand, the internal overvoltage multiplier requirements of EHV system are more stringent, and the ferromagnetic resonance overvoltage may exceed the internal overvoltage level of EHV system. Therefore, the hassle of ferromagnetic resonance in electricity structures is turning into extra and extra prominent, and there is a pressing want to behavior in-depth lookup at the nonlinear traits of ferromagnetic resonance and the suppression of ferromagnetic resonance overvoltage.

A passive (meaning without a separate power supply) linear time-invariant circuit containing an inductor coil and capacitor which, under the action of an applied power supply at a specific frequency, is purely resistive externally. This particular frequency is the resonant frequency of the circuit. To resonate as the main working state of the circuit called resonant circuit. Radio equipment are used to wipe the vibration circuit to complete the tuning, filtering and other functions. The power system is to prevent resonance to avoid bow|overcurrent, overvoltage. The resonance in the circuit are linear resonance, non-linear resonance and parametric resonance. At present, the major characteristics of ferromagnetic resonance assessment and suppression techniques are in predominant based totally completely on the ferromagnetic resonant circuit model, which is received via the use of simplifying the regular ferromagnetic resonant circuit and can replicate the standard legislation of ferromagnetic resonance to a positive extent, laying the foundation for ferromagnetic resonance research. However, the traditional ferromagnetic resonance model requires a precise resonant circuit model and accurate system parameters, and in the actual power system, the resonant circuit and system parameters will change with the change of operation mode, so the characteristic analysis and suppression method based on the traditional ferromagnetic resonance model cannot meet the field application with changing situation.

2 Mechanism of Grid Ferromagnetic Resonance Overvoltage

2.1 Basic Ferromagnetic Resonant Circuit

In order to analyze and discuss ferroresonant overvoltage, first analyze the simplest series resonant circuit. Its equivalent circuit is shown in the figure. L is a nonlinear inductor with an iron core, and C is an equivalent capacitance.

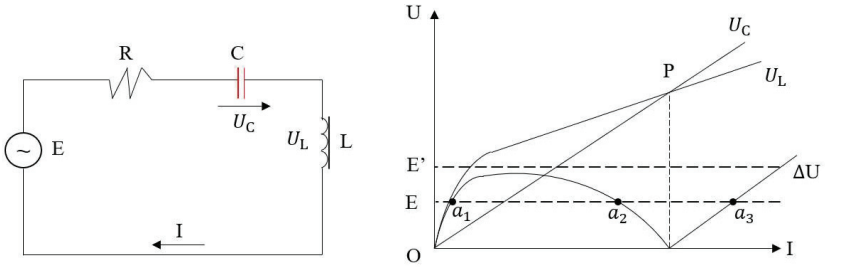

(a)Single-phase series resonant circuits (b) Series ferromagnetic resonant circuit characteristic curve

Figure 1 Single-phase series resonant circuit, characteristic curve.

In order to simplify the analysis and omit the loss (R $=$ 0), when the ferromagnetic resonance occurs, in addition to the fundamental frequency component, there are higher harmonic components, but in the fundamental frequency component, the higher harmonic component does not play a major role, and is ignored in the analysis [5, 6].

According to the circuit in Figure 1(a), the characteristic curves of the voltage of the inductor and capacitor with the circui current $U_L(I)$,$U_C(I)$ can be drawn. Both the voltage and current are shown in the graph as rms values. Since the capacitance is linear, $U_C(I)$ is a straight line [7]. The voltage on the inductor U_L and the voltage on the capacitor U_C have opposite signs. When $\omega L > 1/\omega C$, i.e., when $U_L > U_C$, the current in the circuit is perceptual. However, as the current increases, the core becomes saturated and the inductance decreases, and the two volt-ampere curves intersect at P. The current continues to increase, $U_C > U_L$, and the current in the circuit becomes capacitive.

From the equilibrium relationship between the voltage drop throughout the circuit factors and the electric powered conceivable of the energy provide, it follows that:

$$\dot{E} = \dot{U}_L + \dot{U}_C \tag{1}$$

The above balanced equation can be expressed as the absolute value of the sum of voltage drops ΔU:

$$E = \Delta U = |U_L - U_C| \tag{2}$$

The curve of ΔU versus I can be made from the above equation, as shown in Figure 1(b).

The intersection point of the electric potential and the curve is the point that satisfies the equilibrium Equation (2). As can be seen in Figure 1(b),

there are three equilibrium points a_1, a_2, and a_3, all of which satisfy the equilibrium condition and may become the operating point of the circuit, but all three points are not stable. In physics, a small disturbance can be used to determine the stability of the equilibrium point, assuming that there is a small disturbance in the circuit, and analyze whether this disturbance can make the circuit out of the point [8, 9]. For example, at point a_1, if the current in the loop increases slightly, $\Delta U > E$, i.e., the voltage drop is greater than the electric potential, which reduces the loop current I, and returns to point a_1; conversely, if the current in the loop I decreases slightly, $\Delta U < E$, i.e., the voltage drop is less than the electric potential, which increases the loop current I, and also returns to point $a_{1,}$ so point a_1 is a stable point. Using the same method to analyze points a_2 and a_3, we can find that point a_2 is an unstable point and point a_3 is a stable point.

From the above analysis, it can be viewed that underneath the motion of a sure utilized electric-powered practicable E, there are two steady factors a1 and a3 in the loop, that is, the ferromagnetic resonance loop has two viable secure running states. At point a_1, the circuit is inductive, in a non-resonant state, the voltage on the inductor and capacitor are not high, and the circuit current is not large. At point a_3, the circuit is capacitive, at this time, the inductor and capacitor will produce a high overvoltage, and the circuit current is large, generally said that the circuit is in a resonant working state.

Under regular circumstances, the loop is usually in a non-resonant working state, when the device suffers a robust disturbance, the loop will soar from the a1 factor to the resonant region, this want for the transition method to set up the resonant scenario is known as ferromagnetic resonance excitation, ferromagnetic resonance country can be "self-sustaining", maintained in the resonant state. When the applied power supply E exceeds a certain value, the analysis of Figure 1(b) shows that there is only one working point of the circuit, that is, the circuit works in the resonant state, this situation is called self-excitation phenomenon [10]. When the resistance of the loop is taken into account, the ΔU curve in Figure 1(b) will be shifted upward, and the corresponding excitation resonance requires greater interference, reducing the possibility of resonance and limiting the amplitude of overvoltage.

2.2 Electromagnetic Voltage Transformer Saturation Caused by Overvoltage

The neutral factor is now not a grounded system, in order to display the device's three relative floor voltage, energy metering and relay protection,

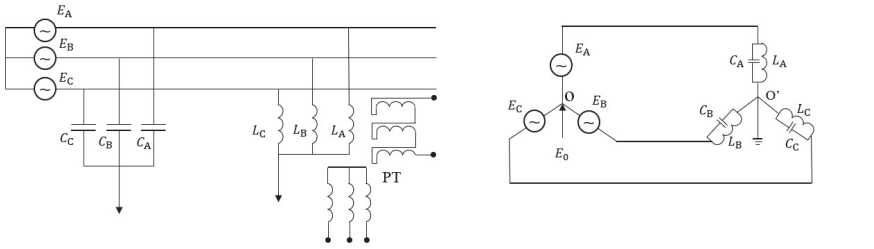

(a) Neutral point ungrounded system with PT wiring diagram (b) Neutral point ungrounded system with PT equivalence diagram

Figure 2 Circuit diagram with PT neutral point ungrounded and equivalent circuit diagram.

electricity station, substation bus often connected with Y_0 connection PT, and system wiring as shown in Figure 2(a), its equivalent circuit as shown in Figure 2(b) [11].

Figure 2 E_A, E_B, E_C for the three symmetrical power potential, PT excitation inductance were L_A, L_B, L_C, each phase conductor and bus capacitance to ground were C_A, C_B, C_C, the conductance of each phase after parallel connection were Y_A, Y_B, Y_C, the principle analysis of the line impedance and transformer iron loss neglected.

In normal operation, the relative capacitance of the power grid $C_A = C_B = C_C = C_0$. The excitation reactance ωL of the transformer is very large, and the phase impedance is mainly based on the capacitance-to-ground C_0 of the conductor $1/\omega C_0$. The three-phase is basically balanced, and the neutral displacement voltage E_0 of the power grid is close to zero, so there will be no overvoltage.

When the system is subject to external disturbances such as operation or fault, the winding of PT is excited by excitation and saturated, usually the degree of saturation of the three-phase winding is different, so that $Y_A = Y_B = Y_C$, so that the three-phase load becomes unbalanced, resulting in a large frequency displacement voltage at the neutral point, which may also provoke resonant overvoltage [12].

(1) Neutral frequency displacement overvoltage

Due to the one of a kind ranges of saturation, the three phases of PT can also generally show up in the following 4 phenomena.

(1) Three phases have different degrees of saturation, but each phase is still a capacitive conductor.
(2) One phase is inductive due to severe saturation, while the other two phases are still capacitive.

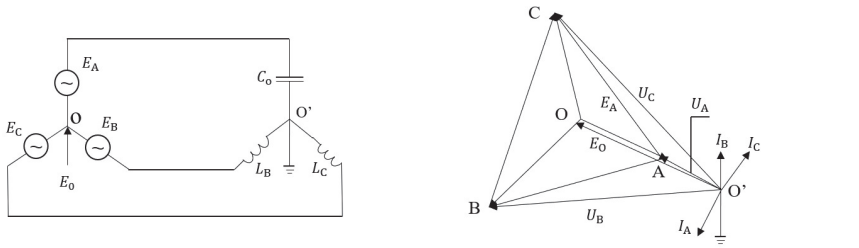

(a) Two-phase saturated equivalent circuit diagram (b) Neutral point displacement is a voltage and current vector diagram

Figure 3 Schematic diagram of system PT core saturation overvoltage.

(3) Two phases are inductive due to severe saturation, and the other – phase is still capacitive.
(4) All three phases are inductive due to severe saturation.

Operation and dimension journey suggests that most of the machine PT core saturation overvoltage for the 0.33 case, that is, two phases due to extreme saturation is inductive, the different segment is nonetheless capacitive, when the two-phase voltage increases, a segment voltage decreases. In this area to analyze the 1/3 case, different instances have similar evaluation methods. Assume that phase A is not saturated, its equivalent capacitance is C_0; B, C two-phase saturation, its equivalent inductance is $L_B = L_C = \mathrm{L}$, neutral displacement voltage is $\dot{E}_0$, equivalent circuit as shown in Figure 3(a).

According to the nodal voltage method there are:

$$\dot{E}_A - \dot{E}_0)Y_A + (\dot{E}_B - \dot{E}_0)Y_B + (\dot{E}_C - \dot{E}_0)Y_C = 0 \tag{3}$$

A transformation of the above equation yields:

$$\dot{E}_0 = \frac{\dot{E}_A Y_A + \dot{E}_B Y_B + \dot{E}_C Y_C}{Y_A + Y_B + Y_C} = \frac{\sum_{i=A}^{c} \dot{E}_i Y_i}{\sum_{i=A}^{c} Y_i} \tag{4}$$

Substituting $Y_A = j\omega C$, $Y_B = Y_C = \frac{1}{j\omega L}$ into Equation (4), respectively, we get:

$$\dot{E}_0 = -\frac{\dot{E}_A(\omega C + \frac{1}{\omega L})}{\omega C - \frac{2}{\omega L}} \tag{5}$$

Where, $\frac{(\omega C + \frac{1}{\omega L})}{\omega C - \frac{2}{\omega L}} \geq 1$, so $\dot{E}_0$ is reversed with $\dot{E}_A$. At this point the neutral point is shifted outside the voltage triangle in order to satisfy the current balance condition $I_A + I_B + I_C = 0$.

Illusory grounding is the signal of PT saturation prompted by means of the frequency displacement voltage, due to exterior elements to make the transformer that a pair of phases no longer saturate is random so that a pair of floor voltage discounts is additionally random [13].

(2) Harmonic resonant overvoltage

The equivalent transformation of Figure 3(a) with Davinan's equivalence law can be obtained as shown in Figure 1(a) for the basic series resonant circuit. External disturbances caused by the saturation of the PT core will produce a series of harmonics, when the parameters with the appropriate will make a harmonic amplification, causing harmonic resonance overvoltage.

Harmonic resonance occurs when the system neutral voltage is harmonic voltage, set the harmonic resonance system zero sequence voltage rms value of E_0, the power supply frequency potential rms value of E, then the three phase to ground voltage rms value is:

$$U = \sqrt{E^2 + E_0^2} \tag{6}$$

It can be seen that the three phase voltages rise simultaneously when harmonic resonance occurs in the system.

2.3 Evolutionary Trend and State Division of Ferromagnetic Resonance Overvoltage

The evolution fashion of ferromagnetic resonance overvoltage in a energy distribution community can be roughly described as follows: due to the excitation of disturbance or fault, the core of PT is saturated, for that reason the inductance fee is reduced, and the ferromagnetic resonance overvoltage is brought on in the case of parameter matching [14, 15]. The evolution trend is shown in Figure 4.

In neutral ungrounded systems, single-phase grounding fault is the most common cause of ferroresonance overvoltage. It is worth mentioning that the single-phase grounding fault is the same as the fundamental frequency ferroresonance overvoltage, which is also caused by the neutral point voltage displacement, and its performance is "two-phase voltage increase, one-phase voltage decrease", if only by the voltage amplitude identification, it is possible to misjudge, can not effectively carry out the risk identification of ferromagnetic resonance overvoltage [16, 17]. Therefore, it is necessary to deeply study its essence and excavate the signal characteristics that can

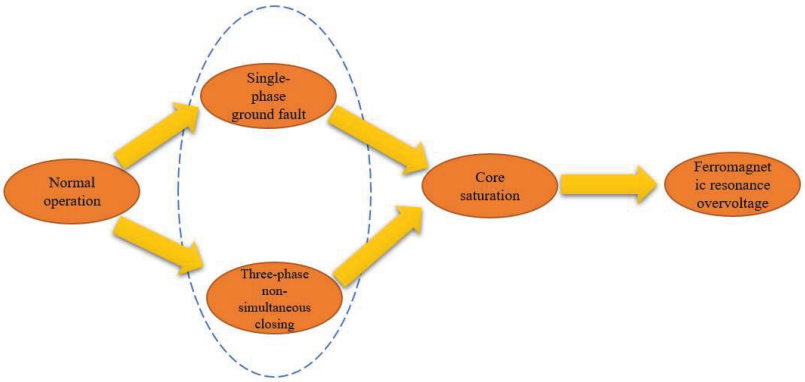

Figure 4 Evolutionary mechanism of ferromagnetic resonance overvoltage.

accurately characterize each state, so as to effectively identify the current state of the distribution network and warn the risks faced in the future period of time.

3 Multi-source Data Fusion for Grid Fault Diagnosis

3.1 D-S Evidence Theory

Suppose the identification frame of the non-empty set is $\Theta = \{x_1, x_2, \ldots, x_n\}$ and its possible subsets are 2^{Θ}. If m: $2^{\Theta} \to [0, 1]$ can satisfy the following equation:

$$\begin{cases} m(\varphi) = 0 \\ \sum_{A \subset \Theta} m(A) = 1 \end{cases} \tag{7}$$

Where: φ denotes an empty proposition.

Then m is called the basic confidence assignment, and for any subset A, then m(A) denotes the basic confidence number of A.

Suppose m_1, m_2, …, m_n denote the basic probabilities in the identification frame Θ, then the following equation holds:

$$m(A) = \begin{cases} 0 & A = \varphi \\ K \sum_{A_i \subset A} m_j(A_i) = 1 & A \neq \varphi \end{cases} \tag{8}$$

Where: $K = [1 - \sum_{A \cap A_i = A} m_j(A_i)]^{-1}$ represents the conflicting weights. When $K < \infty$, it means that the class of evidence is generally

consistent; when $K = \infty$, it means that the class of evidence is contradictory, and the evidence theory is no longer applicable at this time.

3.2 Grid Fault Information Processing

3.2.1 Electrical quantity fault degree

When a fault happens in the grid, the line contemporary earlier than and after the fault takes place adjustments significantly. Therefore, the wavelet fault degree, wavelet singularity degree, and wavelet strength diploma of the electrical present-day sign are defined [18].

(1) Wavelet fault degree

When a fault occurs in the power grid, the fault line current will fluctuate greatly, and the wavelet fault degree of the fault current is defined as follows:

Assume that the fault signal received by the ith component of the grid is $x_i(n)$, and the multiresolution analysis result is $D_{i1}, D_{i2}, \ldots, D_{il}$ by wavelet transform, where l is the number of sampling points of wavelet transform. According to the wavelet transform, the wavelet transform data before the accident is $D_{i1}, D_{i2}, \ldots, D_{ik}, D_{i(k+1)}$, and the wavelet transform data after the fault is $D_{i(k+2)}$. Then let the following equation [19].

$$F_{if} = max(D_{i1}, D_{i2} \ldots D_{ik}) \tag{9}$$

$$F_{ib} = max(D_{i(k+1)}, D_{i(k+2)} \ldots D_{il}) \tag{10}$$

$$V_i = \frac{max(F_{if}, F_{ib})}{min(F_{if}, F_{ib})} \tag{11}$$

In this formula, the basic meaning of V_i is the amplitude of the original signal amplitude change before and after the fault.

In the case of a fault, V_i can be obtained by processing:

$$x_i = \frac{V_i^2}{V_1^2 + V_2^2 + \cdots + V_n^2} \tag{12}$$

Therefore, the above equation represents the wavelet fault degree of component i after the fault.

(2) Wavelet singularity

After the fault occurs, the wavelet radically change converts the authentic sign into the coefficient matrix corresponding to the wavelet transform [20].

According to the simple principle of singularity decomposition, the corresponding singularity decomposition attribute matrix can be obtained, which can additionally symbolize the primary modal characteristics corresponding to the wavelet radically change coefficient matrix.

When a fault happens in the electricity grid, the electrical sign of the misguided issue has a giant quantity of high-frequency transient components, and in contrast with the non-faulty component, the electrical sign of the misguided aspect has a giant change. Assume that the singularity matrix corresponding to the ith issue is.

$$\Lambda_i = \mathrm{diag}(\lambda_1, \lambda_1, \ldots, \lambda_n) \tag{13}$$

Then,

$$S_i = \sum_{i=1}^{l} \lambda_i / t \tag{14}$$

Further processing yields:

$$m_i = \frac{S_i^2}{S_1^2 + S_2^2 + \cdots + S_n^2} \tag{15}$$

(3) Wavelet energy degree

In order to analyze the electricity distribution corresponding to distinctive frequency bands of erroneous electrical signals, wavelet seriously change coefficients can be used as a reference to signify the power signal, then the electricity of the sign electricity can be expressed with the aid of the dimension of the electricity cost [21, 22].

The aforementioned analysis shows that the energy distribution of the wavelet transformed coefficients is $E_1, E_2, \ldots, E_m$, so the processing of Equation (11) can be obtained as follows:

$$W = \sum_{j=1}^{m} E_j / m \tag{16}$$

Further processing yields:

$$e_i = \frac{W_i^2}{W_1^2 + W_2^2 + \cdots + W_n^2} \tag{17}$$

Thus, the expression represents the wavelet energy measure corresponding to x_n signal of component i after the fault.

3.2.2 Switching fault degree

A modified hierarchical weighted fuzzy Petri internet is used to convert the switching portions beneath grid faults to their corresponding issue fuzzy fault degrees, i.e., the line switching portions are transformed into the corresponding numerical portions by means of the modified hierarchical weighted fuzzy Petri net [23]. The Petri net model is constructed for each component, and the fuzzy inference principle is used to obtain the fault probabilities of line components as $p_1, p_2, \ldots, p_n$, respectively, because the sum of the fault probabilities of various components under the fault is not exactly equal to 1, which cannot satisfy the basic fusion rules of the evidence theory. For this reason, the normalization method is used to treat the failure probabilities as follows.

$$g_i = \frac{p_i}{\sum_{j=1}^{n} p_j} \tag{18}$$

Therefore, the processed fault probability matrix $G = \{g_1, g_2, \ldots, g_n\}$ can be expressed as the fuzzy fault degree.

3.3 Fault Diagnosis Decision Method

The basic architecture of the grid fault diagnosis method is shown in Figure 5 by combining the above analysis.

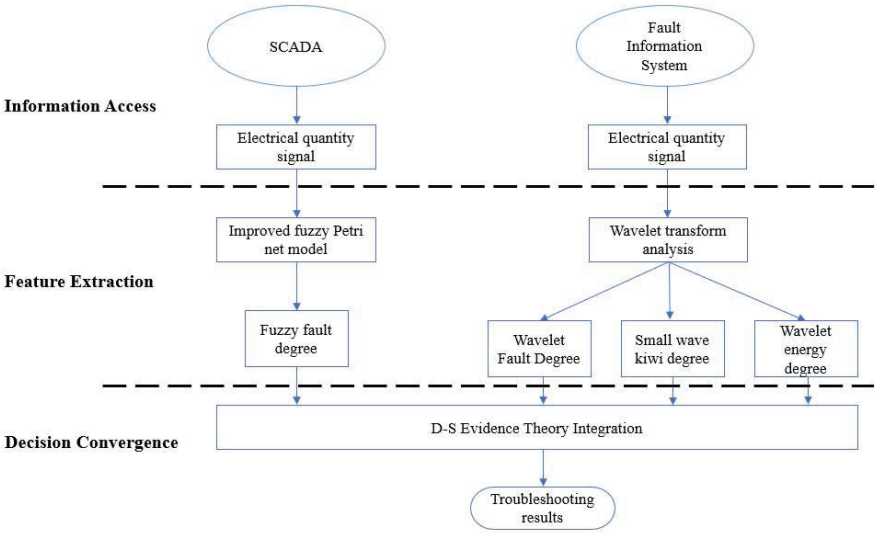

Figure 5 Grid fault diagnosis framework diagram.

The specific steps are as follows:

(1) Fault prognosis data acquisition: the SCADA machine of the electricity grid and the relay safety machine of the electricity grid are used to achieve the switching extent data and electrical extent statistics when the electricity grid is faulty, and in addition search the misguided region of the strength grid to represent the set of misguided components.
(2) Feature extraction: the switching and electrical portions of fault factors are extracted separately, the place the electrical extent data is extracted through wavelet radically changes to analyze the fault contemporary sign in the fault thing set to reap the corresponding wavelet fault degree, wavelet singularity, and wavelet power degree, which are used to signify the fault probability; whilst the switching volume records is extracted by using multiplied hierarchical weighted fuzzy Petri. The swap facts aspects are extracted the usage of a modified hierarchical weighted fuzzy Petri internet to technique and analyze the change portions and reap the corresponding fuzzy fault diploma to the components [24].
(3) Decision fusion: According to the multi-source statistics such as the electrical extent and switching quantity, the D-S proof principle algorithm is used to fuse the electrical volume facts and switching extent information, and the misguided aspects can be received in accordance with the fault analysis selection method, so as to acquire the fault prognosis outcomes.

4 Research on Active Distribution Network Operation Risk Warning by Multi-source Data Analysis

4.1 Probability Distribution Model of Wind Power Load Prediction Error

In addition, there is a positive error between the envisioned and proper wind electricity values due to the uncertainty of wind electricity and the hassle of the prediction technique itself, therefore, it is of sensible magnitude to learn about the likelihood density distribution feature of wind energy prediction error.

The wind power prediction error probability distribution generally conforms to a non-standard normal distribution, as shown below.

$$f_w(x) = \frac{1}{\sqrt{2\pi}\sigma_w}\exp\left(-\frac{x^2}{2\sigma_w^2}\right) \tag{19}$$

$$\sigma_w = (a + b \times w_f)P_w \tag{20}$$

4.2 EV Probability Distribution Model

The consequences of the 2009 U.S. Department of Transportation survey of family motors throughout the U.S. have been used, and the statistics from them had been normalized and then processed the use of the approach of splendid possibility estimation. The vehicle's first day out second and the final day trip return second are approximated as ordinary distributions, and the everyday mileage is approximated as a log-normal distribution [25, 26].

The return moment, i.e., the moment when the user drops off the EV at the EV charging station to start charging, satisfies a normal distribution with a probability density function of:

$$f_{\mathrm{e}}(x) = \begin{cases} \dfrac{1}{\sigma_e\sqrt{2\pi}} e^{\left(-\frac{(x-\mu_{e2})^2}{2\sigma_e^2}\right)} & 0 < x \le \mu_e + 12 \\ \dfrac{1}{\sigma_e\sqrt{2\pi}} e^{\left(-\frac{(x-24-\mu_e)^2}{2\sigma_e^2}\right)} & \mu_e + 12 < x \le 24 \end{cases} \tag{21}$$

The daily mileage follows a log-normal distribution with a probability density function of:

$$f_D(x) = \frac{1}{x\sigma_D\sqrt{2\pi}} e^{\left(-\frac{(\ln x-\mu_D)^2}{2\sigma_D^2}\right)} \tag{22}$$

Assuming that the EV is charged with constant power, its charging power distribution, i.e.

$$f_{P_c}(x) = \begin{cases} P_c & x_s \le x \le x_e \\ 0 & \text{else} \end{cases} \tag{23}$$

To simplify the analysis, some assumptions are made in this paper, as follows:

(1) EVs that enter the station at [t, t + 1] are considered to start charging from time slot t + 1.
(2) After the EV starts charging, the charging process continues until the end.

4.3 Distribution Network Operation Risk Warning Mechanism

The core task of distribution network operation risk warning is to accurately identify the network risk factors, and through risk analysis and assessment of their severity, so as to determine its risk level. Issue warnings according

to the level of risk. Therefore, the key technologies to realize the distribution network operation risk early warning include the distribution network time series operation risk assessment calculation and risk grading method and the time period early warning based on risk grading. In the following chapters, it is explained separately.

4.3.1 Time-series risk analysis of the distribution network

Time-series threat evaluation of the distribution community is a danger evaluation via calculating hazard warning signs for distinctive moments of the distribution community inside a day in chronological order. Since dangers are additionally combinable in time, in this paper, on the foundation of area 3.2, we advise the time-level chance warning signs as proven in Figure 6. At the temporal level, the calculated distribution community built-in danger below every second is superimposed to acquire the built-in chance of the distribution community underneath the comparison cycle [27].

(1) Calculation of risk indicators at the moment t

For all scenarios the tidal current calculation is performed to obtain the distribution of voltage and line power. The overvoltage probability and severity are calculated, and then the overvoltage operation risk of the node is obtained, as

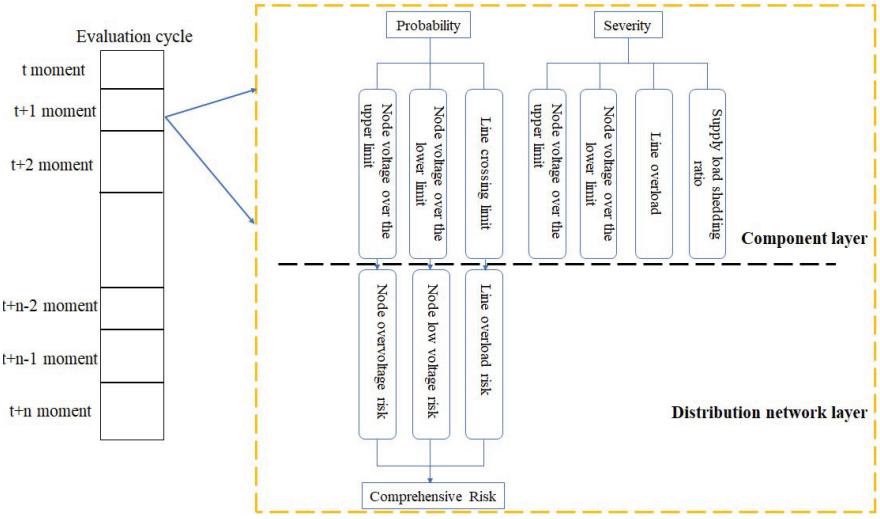

Figure 6 Spatio-temporal two-level distribution network risk index system.

shown in Equation (24):

$$R_{i,t}^{vh} = \sum_{s \in \Omega^t} \rho_{t,s} B_{i,t,s}^{vh}(V_{i,t,s}) \mathrm{Sev}^{vh}(V_{i,t,s}) \forall i, \forall t \tag{24}$$

Where, $R_{i,t}^{vh}$ is the overvoltage risk of the ith node at time t; Ω is the set of generated operation scenarios at time t.

(2) The set of operational risk indicators of the distribution network at moment t can be calculated by combining the low voltage and overvoltage operational risks of each node at time t and the overload operational risk of each line respectively, as shown below:

$$R_{sys,t}^{vh} = \sum_{i=1}^{N_b} w_i R_{i,t}^{vh} \tag{25}$$

$$R_{sys,t}^{vl} = w_i \sum_{i=1}^{N_b} R_{i,t}^{vl} \tag{26}$$

$$R_{sys,t}^{p} = \sum_{j=1}^{N_t} R_{j,i}^{p} \tag{27}$$

$$\begin{cases} R_{\mathrm{load},t}^{vh} = \sum_{i=1}^{N_b} \sum_{s \in \Omega^t} \rho_{t,s} B_{i,t,s}^{vh}(V_{i,t,s}) P_{\mathrm{load}}^{vh} \forall i, \forall t \\ R_{\mathrm{load},t}^{vl} = \sum_{i=1}^{N_b} \sum_{s \in \Omega^t} \rho_{t,s} B_{i,t,s}^{vl}(V_{i,t,s}) P_{\mathrm{load}}^{vl} \forall i, \forall t \\ R_{\mathrm{load},t}^{p} = \sum_{j=1}^{N_l} \sum_{s \in \Omega^t} \rho_{t,s} B_{j,t,s}(P_{j,t,s}) P_{\mathrm{load}}^{p} \forall i, \forall t \\ R_{\mathrm{load},sys}^{t} = max\{R_{\mathrm{load},t}^{vh}, R_{\mathrm{load},t}^{vl}, R_{\mathrm{load},t}^{p}\} \end{cases} \tag{28}$$

$R_{sys,t}^{vh}$ is the distribution network overvoltage operation risk at time t; $R_{sys,t}^{vl}$ is the distribution network undervoltage operation risk at time t; $R_{sys,t}^{p}$ is the distribution network line overload operation risk at time t; $R_{\mathrm{load},t}^{vh}$, $R_{\mathrm{load},t}^{vl}$ and $R_{\mathrm{load},t}^{p}$ are the distribution network loss of load operation risk

caused by voltage overrun and line overload, respectively. $R^t_{\text{load},sys}$ is the risk of loss of load operation of distribution network caused by voltage overrun and line overload [28, 29].

(3) The daily distribution network operation risk can be calculated by accumulating the comprehensive risk of each time period as follows:

$$R^{vh}_{sys} = \sum_{t=1}^{T} R^{vh}_{sys,t} \tag{29}$$

$$R^{vl}_{sys} = \sum_{t=1}^{T} R^{vl}_{sys,t} \tag{30}$$

$$R^{p}_{sys} = \sum_{t=1}^{T} R^{p}_{sys,t} \tag{31}$$

$$R^{\text{load}}_{\text{sys}} = \sum_{t=1}^{T} R^{\text{load}}_{\text{sys},t} \tag{32}$$

Where, R^{vh}_{sys} is the daily distribution network overvoltage operation risk; R^{vl}_{sys} is the daily distribution network undervoltage operation risk; R^{p}_{sys} is the daily distribution network line overload operation risk; $R^{\text{load}}_{\text{sys}}$ is the daily distribution network loss of load operation risk.

(4) Calculate the integrated operation risk of distribution network

$$CRI = w_1 R^{vh}_{sys} + w_2 R^{vl}_{sys} + w_3 R^{p}_{sys} + w_4 R^{\text{load}}_{sys} \tag{33}$$

4.3.2 Distribution network risk warning criteria

After the time collection danger evaluation of the distribution community a few days ago, this paper divides the distribution community hazard level, danger place and node threat diploma by means of sure rules. According to the effects got from the classification, the early warning data is despatched to the dispatching area to become aware of the hazard degree of the distribution community in every time period, medium and excessive danger areas (lines and nodes), etc. The precise guidelines of distribution community hazard warning are as follows.

Table 1

Risk Level	Grading Criteria
Red level (highest risk)	$P_{load} > 30\%$
Orange level (higher risk)	$10\% < P_{load} = 30\%$
Yellow level (medium risk)	$4\% < P_{load} = 10\%$
Green level (low risk)	$P_{load} = 4\%$

(1) Risk level warning

Although complete warning signs can assist operators to have a complete perception of distribution community risks, it can additionally be tough to choose, in the end, which indicator to use. Classification standards must be developed to decide precise hazard stages to convey extra comfort to information operators' operations. According to the Safety Accident Investigation Protocol of the State Grid Corporation, the distribution network risk is divided into 4 levels according to the load shedding ratio, with reference to the weather warning selected as red, orange, yellow and green representing low risk, medium risk, higher risk and high risk respectively, as shown in Table 1.

(2) Risk point warning

According to the minimum reasonable and feasible guidelines, combined with the "State Grid Corporation Safety Accident Investigation Regulations" set the risk demarcation line, thus dividing the node overvoltage risk, node low voltage risk value to determine the medium and high risk nodes.

4.3.3 Distribution network risk early warning process

The charging power of EV charging stations is simulated using Monte Carlo simulation in the following sub-steps:

(1) Simulate the starting charging moment, leaving period, and daily driving kilometers respectively according to the EV probability model.
(2) EV charging time T_e is calculated according to the daily mileage D and the charging amount W_{100} required for EV 100 km mileage, as shown below:

$$T_g = \frac{DW_{100}}{100P_c} \tag{34}$$

(3) Repeat the above steps for each EV;
(4) Obtain the hourly charging power of the charging station by accumulating the charging power of each EV;

4.4 Analysis of Calculation Example

Since the wind velocity and mild in a day lead to special PV and wind turbine output at exclusive moments, the usage of the suggest fee has limitations, so it is very crucial to analyze the hazard of distribution community operation below specific hours of the day to grant choice groundwork and help for the dispatch of a day. In this paper, primarily based on IEEE34 distribution system, two get entry to scenarios, DG and DG&EV, are set to analyze the distribution community for timing operation hazard and early warning lookup respectively [30].

4.4.1 Timing operation risk analysis and early warning of distribution network under DG access

According to the influence evaluation in the preceding section, the get right of entry to situation of DG adopted by means of IEEE34 distribution machine is proven in Figure 7, in which two wind generators are related at node 15, node 34 is linked with wind energy complementary, and node 33 is related with one wind turbine. Based on the regular load demand, wind turbine and PV lively output prediction curves, the envisioned values of every time duration are transformed into corresponding ratios primarily based on the respective expected peaks, and the energetic output ratio coefficients of load demand, WT and PV for every time duration earlier than the day are obtained, as proven in Figure 8. The error earlier than the wind and mild load day is set to 20%.

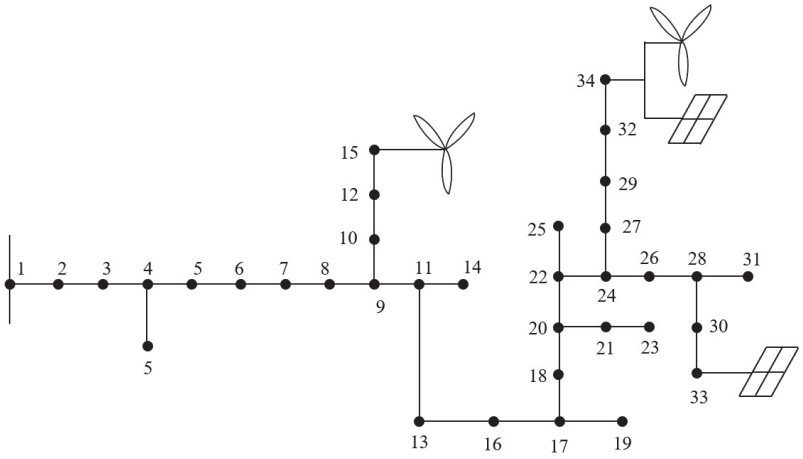

Figure 7 Wiring diagram of IEEE34 system with DG.

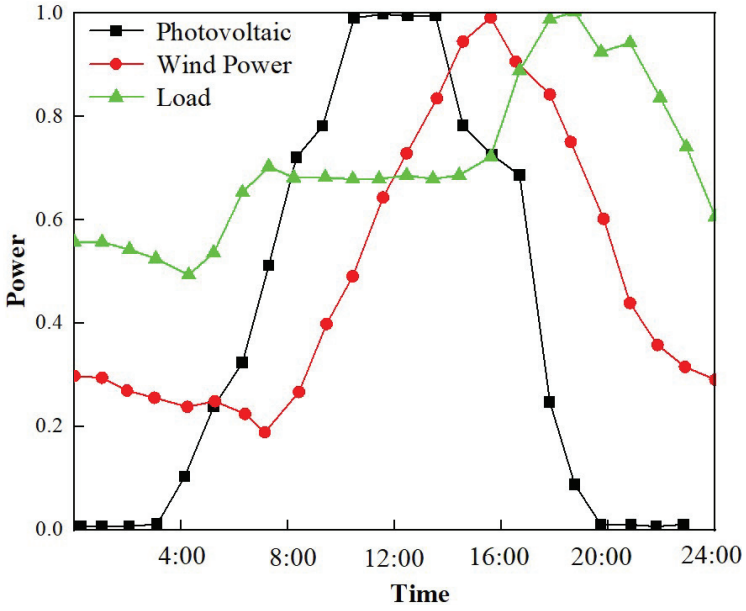

Figure 8 Proportional coefficients of active output of load demand, WT and PV for each time period before the day.

(1) Time-series operation risk analysis

The values of each risk index in the distribution network during the evaluation cycle are shown in Figure 9. The risk of distribution network is mainly composed of overvoltage risk and risk of loss of load operation caused by overvoltage. As can be seen from the figure, the risky hours of the distribution network are concentrated in the period from 9:00 to 20:00, which is due to the fact that the DG output power is above 50% during this period, and the distribution network load cannot completely consume the DG output power, thus leading to the voltage crossing the upper limit. Due to the limitation of light conditions and wind speed, the DG output in the evening of the distribution network is smaller, and the corresponding distribution network over-voltage operation risk is smaller [31].

Further, the overvoltage operation risk of each node in the distribution network during a day is analyzed, as shown in Figure 9. The over-voltage risk of each node in the distribution network is ranked at each node (#33, #34, #15) and nearby nodes (#12). This is due to the fact that the PV output is 0 at night due to the natural lighting conditions, but there are still nodes

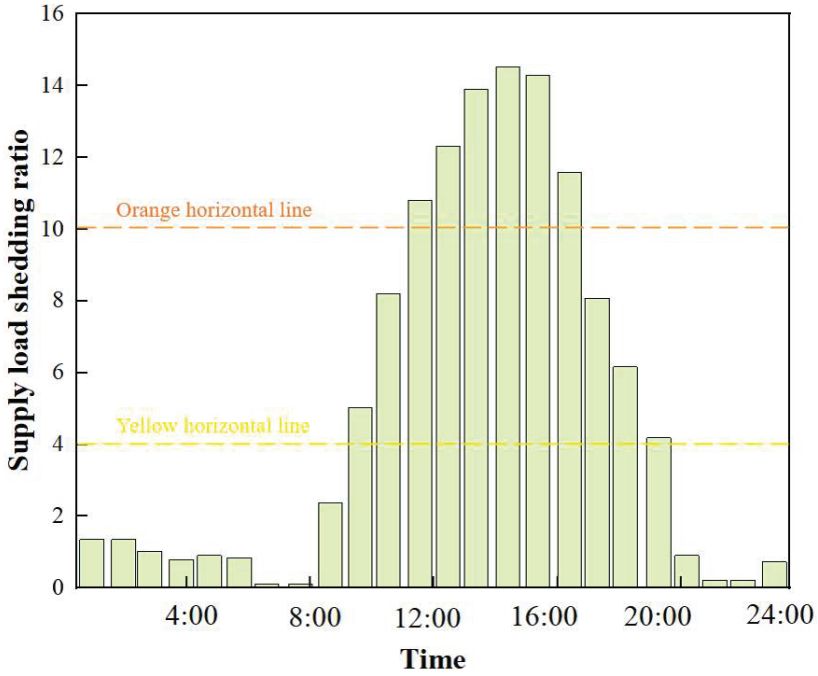

!

Figure 9 Risk level warning in the distribution network assessment cycle.

with wind turbines feeding power backwards to the surrounding area, which leads to the voltage rise in the area. In summary, the distribution network risk containing DG is mainly affected by the DG output of one day.

(2) Day-ahead warning analysis

According to the day-ahead risk assessment index, the risk warning of each time period of the distribution network is shown in Figure 9. According to the early warning results, the dispatcher should pay close attention to monitoring the distribution network overvoltage during the period from 9:00 to 20:00, especially from 12:00 to 17:00, when the distribution network is at orange risk. The medium and high risk areas of the distribution network vary from time to time and are mainly concentrated in the central and tail nodes of the distribution network. Therefore, dispatchers can take timely measures to reduce the risk of the distribution network during the medium and high risk periods, such as reducing the DG output and other measures. The reduction of DG output is actually an economic loss.

4.4.2 Timing analysis and early warning of distribution network timing operation risks under DG and EV access

Based on the study of risk assessment and risk warning of DG access to the distribution network in Section 4.4.1, this paper adds EV to study the impact of its multiple risk factors on the distribution network risk factors. The locations of scenery access and EV access in the distribution network are shown in Figure 10. Among them, EV charging station is connected to 23 nodes and the charging station contains 200 EVs.

(1) Time-series risk analysis

After the timing risk assessment, it is known that the distribution network appears different risk characteristics in a day due to the changes of DG output and EV charging power in each time period. Overvoltage risk mainly occurs during daytime hours (9:00-17:00), while line overload risk occurs in the distribution network during part of the evening hours (18:00-22:00), where low voltage risk occurs in the distribution network at 21:00 hours. At the same time, the distribution network is at risk of loss of load during all these hours. The distribution network experienced overvoltage risk due to the overlap between EV charging station charging and evening peak load, which caused a certain probability of power supply shortage, and thus the distribution network experienced line overload and low-voltage risk.

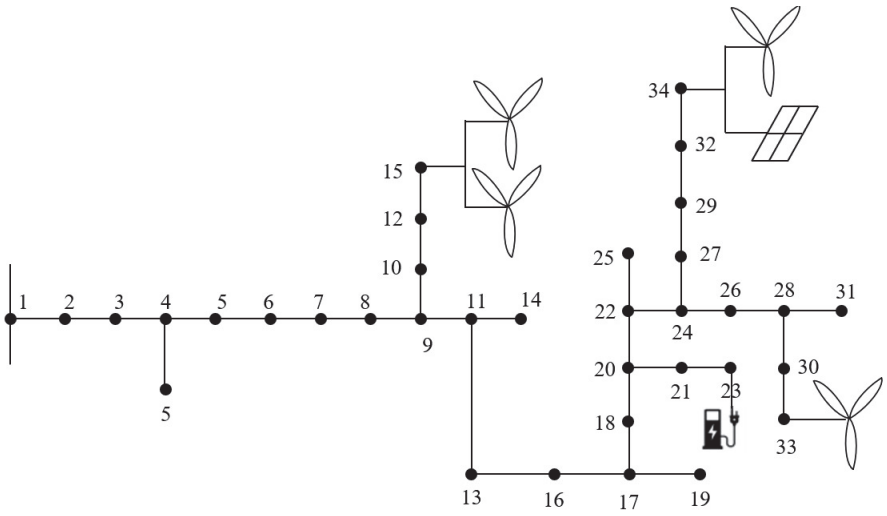

Figure 10 IEEE34 node distribution system with DG and EV.

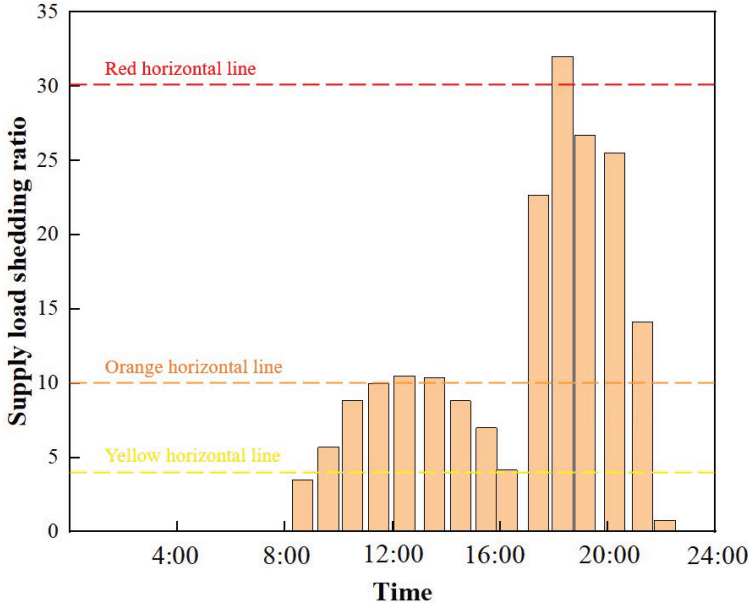

Figure 11 Distribution network warning time map.

(2) Day-ahead warning analysis

According to the day-ahead risk assessment index, the risk warning for each time period of the distribution network is shown in Figure 11. According to the warning results, the time periods when the distribution network is at medium-high risk level increases, and the dispatchers should pay attention to the voltage situation and line overload during the evening hours (19:00-23:00), especially at 19:00 when the distribution network is at red risk. Therefore, according to the above warning map, dispatchers can keep track of the time periods and areas where the potential risks of the distribution network appear. Measures can be taken for the distribution network during medium and high risk periods, such as reducing DG output and adjusting EV charging periods to achieve risk reduction.

5 Conclusion

With the big get right of entry to of disbursed energy sources, the booming improvement of electric powered automobiles and the reform of energy market, the uncertainties in distribution networks are increasing. With this as the beginning point, this paper has performed a learn about on the chance

evaluation and early warning of the lively distribution community below a couple of uncertainties. The essential effects and conclusions are as follows:

(1) The characteristics of fault current information are extracted by wavelet transform, and the corresponding fault degree of electrical volume, such as wavelet fault degree, wavelet singularity degree and wavelet energy measure are obtained respectively. The quantity of switches in fault process is analyzed by fuzzy Petri net. The fuzzy fault degree of the switching signal in the fault process is obtained. Then, the D-S evidence theory is used to fuse the multi-source information of electricity volume and switching quantity, so that the comprehensive fault results of power grid can be obtained more accurately.
(2) The mechanism of the generation of ferromagnetic resonance overvoltage is studied, and the principle of saturation-induced neutral point voltage shift and ferromagnetic resonance, and the principle of wire break-induced ferromagnetic resonance are analyzed by graphical and mathematical analysis, and the current status of research on the classification of ferromagnetic resonance, phenomena and other laws are summarized.
(3) According to the early warning outcomes of IEEE 34 distribution system, in the case of DG access, dispatchers need to pay shut interest to screen the distribution community overvoltage at some stage in the duration of 9:00-20:00, in particular from 12:00 to 17:00 when the distribution community is at orange risk. In the case of DG & EV joint access, the time duration when the distribution community is at medium-high threat stage increases, and dispatchers have to pay interest to the voltage state of affairs and line overload for the duration of the nighttime hours (19:00-23:00), specifically 19:00, when the distribution community is at purple risk.

References

[1] Li W. Risk assessment of power systems: models, methods, and applications[M]. John Wiley & Sons, 2014.
[2] Liu N, Wu T, Xu T, et al. Reliability evaluation method for distribution network[J]. The Journal of Engineering, 2017, 2017(13): 1771–1776.
[3] Perninge M, Soder L. A stochastic control approach to manage operational risk in power systems[J]. IEEE Transactions on Power Systems, 2011, 27(2): 1021–1031.

[4] Hua L, JiRan Z, Haiguo T, et al. Risk assessment for distribution systems based on key performance indicator[C]//2017 IEEE 3rd Information Technology and Mechatronics Engineering Conference (ITOEC). IEEE, 2017: 745–749.

[5] Guo Chuangxin, Lu Haibo, Yu Bin, et al. Summary of research on safety risk assessment of secondary power systems [J] Grid Technology, 2013, 37 (1): 112–118.

[6] Xing Haijun, Cheng Haozhong, Zhang Shenxi, et al. Overview of Research on Active Distribution Network Planning [J] Grid Technology, 2015, 39 (10): 2705–2711.

[7] Li Xinlei Modeling of personnel risk factors during power grid dispatch operations [J] China Science and Technology Journal Database Industry C, 2016 (12): 00272–00272.

[8] Ciapessoni E, Cirio D, Kjølle G, et al. Probabilistic risk-based security assessment of power systems considering incumbent threats and uncertainties[J]. IEEE Transactions on Smart Grid, 2016, 7(6): 2890–2903.

[9] Nagaraj R, Murthy D T, Rajput M M. Modeling Renewables Based Hybrid Power System with Desalination Plant Load Using Neural Networks[J]. Distributed Generation & Alternative Energy Journal, 2019, 34: 32–46.

[10] Liu Tao, Yan Yipeng, Lin Jikeng Analysis of Ferromagnetic Resonance during Black Start of Power Grid [J] Journal of Power Systems and Automation, 2012, 24(2): 90–95.

[11] Semero Y K, Zhang J, Zheng D, et al. A GA-PSO hybrid algorithm based neural network modeling technique for short-term wind power forecasting[J]. Distributed Generation & Alternative Energy Journal, 2018, 33(4): 26–43.

[12] Huang S J, Hsieh C H. Relation analysis for ferroresonance of bus potential transformer and circuit breaker grading capacitance[J]. International Journal of Electrical Power & Energy Systems, 2013, 51: 61–70.

[13] Sendilvelan S, Bhaskar K. Experimental Analysis of Partially Premixed Charge in a Diesel Engine with Jatropha Oil Methyl Ester and Diesel Blends[J]. Distributed Generation & Alternative Energy Journal, 2019, 34(1): 47–60.

[14] Mokryani G, Siano P, Piccolo A. Identification of ferroresonance based on S-transform and support vector machine[J]. Simulation Modelling Practice and Theory, 2010, 18(9): 1412–1424.

[15] Xie Jia'an, Li Tianyun, He Jianwei, et al. Application of HHT in Identification of Ferromagnetic Resonance Overvoltage [J] Power Automation Equipment, 2009, 29 (1): 75–78.
[16] Jiang Jie, Zhao Guangquan, Zhang Xiao, et al. Identification of ferroresonance and single-phase grounding using sine fitting method [J] Journal of Chongqing University: Natural Science Edition, 2014, 37(8): 34–40.
[17] Teron A C, Bartlett A, Duan N, et al. Estimating the nonlinear oscillation frequency of a power system using the harmonic balanced method[C]//2016 IEEE Power and Energy Society General Meeting (PESGM). IEEE, 2016: 1–5.
[18] Jiang Y, Jiang Y, Mu L, et al. An effective method to limit resonance overvoltage caused by single phase grounding fault in ultra-high voltage AC system[C]//2015 IEEE Advanced Information Technology, Electronic and Automation Control Conference (IAEAC). IEEE, 2015: 1210–1214.
[19] Wang Zhiqiang, Li Xin, Li Yan, et al. Comprehensive vulnerability assessment of power grids based on complex networks and risks [J] Modern Electric Power, 2014, 31 (3): 49–55.
[20] Cheng Jiatang, Aili, Duan Zhimei Research on Integrated Fault Diagnosis of Hydroelectric Units Based on Improved D-S [J] Journal of Hydroelectric Power, 2014, 33(5): 216–220.
[21] Gu Kaikai, Guo Jiang Transformer fault diagnosis based on compact fusion of fuzzy sets and fault tree analysis [J] High Voltage Technology, 2014, 40(5): 1507–1513.
[22] Lv Rui, Sun Linfu Fault diagnosis method of complex system based on multi-source information fusion fault tree analysis and fuzzy Petri net [J] Computer Integrated Manufacturing Systems, 2017, 23 (8th): 1817.
[23] Krizhevsky A, Sutskever I, Hinton G E. Imagenet classification with deep convolutional neural networks[J]. Communications of the ACM, 2017, 60(6): 84–90.
[24] Jiang Y, Li L, Liu Z. A multi-objective robust optimization design for grid emergency goods distribution under mixed uncertainty[J]. IEEE Access, 2018, 6: 61117–61129.
[25] Rudin C, Waltz D, Anderson R N, et al. Machine learning for the New York City power grid[J]. IEEE transactions on pattern analysis and machine intelligence, 2011, 34(2): 328–345.
[26] Liu Yunpeng, Xu Ziqiang, Li Gang, et al. Overview of the Application of Artificial Intelligence Driven Data Analysis Technology in

Condition Based Maintenance of Power Transformers [J] High Voltage Technology, 2019 (2): 337–348.
[27] Post M, Bergsma S. Explicit and implicit syntactic features for text classification[C]//Proceedings of the 51st Annual Meeting of the Association for Computational Linguistics (Volume 2: Short Papers). 2013: 866–872.
[28] Yang Zhichun, Shen Yu, Yang Fan, et al. Distribution transformer transfer learning fault diagnosis model considering multi factor situation evolution [J] Journal of Electrical Engineering Technology, 2019, 34(7): 1505–1515.
[29] Zhang Y, Wallace B. A sensitivity analysis of (and practitioners' guide to) convolutional neural networks for sentence classification[J]. arXiv preprint arXiv:1510.03820, 2015.
[30] Dai Jiejie, Song Hui, Sheng Gehao, et al. Research on the Prediction Method of Power Transformer Operation State Using LSTM Network [J] High Voltage Technology, 2018, 44(4): 1099–1106.
[31] Chen L, Liu L, Peng Y, et al. Distribution network operational risk assessment and early warning considering multi-risk factors[J]. IET Generation, Transmission & Distribution, 2020, 14(16): 3139–3149.

Biography

Gou Yu graduated from the College of Electrical Engineering & New Energy at China Three Gorges University, majoring in intelligent electrical information engineering. She has received the Special Scholarship from China Three Gorges University and the Yangtze River Power Scholarship. She won the first prize in the 2022 Hubei iCAN International Innovation China Qualification Competition. Silver Award in the Hubei Province "Challenge Cup Entrepreneurship Competition". Her team won first prize in the 9th National Securities Investment Simulation Training Competition. The main research direction is power system optimization.